FPRINT-94-06

ADAPTIVE SMOOTHED PARTICLE HYDRODYNAMICS AND GALAXY FORMATION [1]

Paul R. Shapiro,[2] Hugo Martel,[2]

and Jens V. Villumsen,[3]

[1] To appear in *Numerical Simulation in Astrophysics*, ed. J. J. Franco (1994) (Cambridge: Cambridge University Press), in press

[2] Department of Astronomy, University of Texas, RLM Hall, Austin, TX 78712, USA.

[3] Department of Astronomy, Ohio State University, Columbus, OH 43210, USA.

Adaptive Smoothed Particle Hydrodynamics and Galaxy Formation

Paul R. Shapiro * *Hugo Martel* * *Jens V. Villumsen* †

Abstract

The development of a new Smoothed Particle Hydrodynamics (SPH) method, called Adaptive Smoothed Particle Hydrodynamics (ASPH), generalized for cosmology and coupled to the Particle Mesh (PM) method for solving the Poisson Equation, for the simulation of galaxy and large-scale structure formation, will be described. The accurate numerical simulation of the highly nonlinear phenomena of shocks and caustics which occur generically in the process of structure formation requires enormous dynamic range and resolution. Previously existing numerical methods require substantial modification in order to achieve the required resolution with current computer technology. The ASPH method incorporates new, adaptive, anisotropic smoothing and shock-tracking algorithms, which significantly enhance the resolving power of the SPH method. We describe tests of ASPH versus SPH against the difficult cosmological pancake collapse problem. All cosmological hydro methods should be required to reproduce this test. High resolution 2D simulations of galaxy and large-scale structure formation in the Hot Dark Matter (HDM) model are presented using ASPH, showing that ASPH can resolve pancake shocks with fewer than 40 particles per pancake per dimension.

1. Introduction

What must the capabilities of a successful cosmological hydro method be? Most theories of galaxy formation assume that structure formed when initially small amplitude, primordial density fluctuations grew by gravitational instability to nonlinear amplitude[1]. Such primordial density fluctuations and gravitational instability lead to gravitational collapse, strong shocks, and radiative cooling, occurring over an enormous range of mass and length scales. Shocks, in fact, are the principal mechanism by which gravitational motions are dissipated so as to make formation of bound, star forming objects possible.

Nearly 1D, plane-symmetric collapse to form structures known as cosmological pancakes is a generic feature of the nonlinear growth of a 3D spectrum of density fluctuations. While more complicated structures also arise, the pancakes provide us with an example of a minimally complicated flow which all cosmological hydro methods must be capable of reproducing.

*Department of Astronomy, University of Texas, Austin, TX 78712, USA. We acknowledge NASA NAGW-2399, Robert A. Welch F-1115, the UT System Center for High Performance Computing and the NSF NCSA.

†Department of Astronomy, Ohio State University, Columbus, OH 43210, USA. We acknowledge the Ohio Supercomputer Center.

1D pancake calculations[2] show that, in the absence of radiative cooling, a dynamic range of more than 10^3 in density and in length scale is required to resolve even a single pancake. *With* radiative cooling, the dynamic range increases to more than 10^5.

Are existing numerical hydro methods adequate? No. In order to achieve the dynamic range described above, necessary to follow randomly oriented pancake collapse, a 3-D, Eulerian grid (i.e. fixed spatial grid, uniformly spaced, nonadaptive mesh) must have more than 10^3 cells *per dimension*, or 10^9 cells, *per pancake* for simulations *without* radiative cooling and more than 10^5 cells *per dimension*, or 10^{15} cells, *per pancake with* radiative cooling! Current Eulerian methods are limited by existing hardware to $\approx 10^2$ cells per dimension.

Existing Lagrangian hydro methods such as SPH would seem to be a more promising alternative, since they, in principle, adjust their resolution dynamically to follow the flow. Cosmology simulations with SPH have typically used a number of particles $N_{gas} \sim 32^3$ or less, however. (Simulations with $N_{gas} = 64^3$ have recently been reported, but with dynamic range limited by imposing a minimum smoothing length.) As we shall demonstrate, this limitation and the requirement that artificial viscosity be used to treat shocks has kept the capabilities of this method below the level required.

In what follows, we describe the development of a new version of SPH called *Adaptive* SPH (ASPH) which greatly enhances the dynamic range and resolving power of SPH to levels which promise to resolve the shocks which are generic to galaxy and large-scale structure formation flows.

2. Standard Smoothed Particle Hydrodynamics (SPH)

The SPH method[3] is a Lagrangian numerical hydrodynamics method which replaces the continuous baryon-electron fluid by a set of discrete gas "particles" which carry mass and thermal energy and move with the local flow velocity. The particles are essentially moving centers of interpolation for representing the continuous flow variables. As such, they eliminate the need for a numerical grid or the interpolation back and forth between particles and grid. The principal virtue of this method is that, as a Lagrangian method, it has numerical resolution which dynamically adjusts so as to follow the compression, expansion, and distortion of the flow. It has demonstrated great success in a wide variety of astrophysical flow applications.

Isotropic Smoothing Length. The resolving power of the SPH method is related to the "smoothing length" h used for its interpolations, which defines a spherical "zone of influence" centered on each particle. Initially, this $h = h_0$, the mean interparticle spacing (or twice this). In order for the resolution to adjust dynamically to accommodate a changing gas density, the smoothing length must vary in time and space as a function of that density. Ideally, the variations of h should be such as to maintain a constant number of "nearest neighbor" particles, those within a distance of only a few smoothing lengths or less from a given particle. The interpolations which SPH performs in order to evaluate fluid quantities and their gradients anywhere within the computational volume involve sums over the values of those quantities known at the irregularly spaced positions of these "nearest neighbor"

particles, weighted by a kernel function W, an isotropic function of the smoothing length, or its gradient. For an isotropic Gaussian kernel W in 3D,

$$W(\mathbf{r}_i - \mathbf{r}_j, h) = \pi^{-3/2} h^{-3} \exp(-r_{ij}^2/h^2)\,, \tag{1}$$

where h is a scalar which varies in space and time according to one of two choices,

$$h = h_p = h_0(\rho_p/\rho_0)^{-1/3} \qquad p = i \text{ or } j\,, \tag{2}$$

where ρ_i and ρ_j are the density evaluated at the location $\mathbf{r}_i = (x_i, y_i, z_i)$ of particle i and the location $\mathbf{r}_j = (x_j, y_j, z_j)$ of particle j, respectively, $r_{ij} = |\mathbf{r}_i - \mathbf{r}_j|$, and ρ_0 is the initial mean density. The "nearest neighbor" particles are taken to be all those within a distance $r_{ij} \leq 3h$ of particle i.

Artificial Viscosity. Artificial viscosity must be introduced in the standard SPH equations in order to prevent particle trajectory crossing and allow shocks to form.

3. Adaptive Smoothed Particle Hydrodynamics (ASPH)

Standard SPH suffers from the following two limitations which become particularly serious in the generic flows which occur in the formation of galaxies and large-scale structure, involving gravitational collapse through orders of magnitude of compression and strong shock waves:

1) The isotropic variable smoothing length is valid for nearly isotropic compressions or expansions, but breaks down in the presence of strongly anisotropic compression such as in pancake collapse.

2) Shocks require artificial viscosity, but gravitational collapse then results in false "preheating" of supersonically infalling gas, far outside of the actual shock location. This artificially spreads out the shock-heating and can be disastrous for calculations which include radiative cooling, for example.

We solve these problems by (1) replacing the isotropic kernel and smoothing length by a fully adaptive, *anisotropic kernel* and *tensor smoothing length* $\mathbf{H}$ which tracks the anisotropy of fluid motions; and (2) *tracking the shock* and *restricting the viscous heating to particles at the shock*, as described below.

Anisotropic smoothing tensor $\mathbf{H}$. In standard SPH, the zone of influence of a given particle is a sphere centered on that particle, with a radius of order a few smoothing lengths. The spatial resolution in this region of the fluid is given by the smoothing length, and is therefore isotropic. However, in situations involving strong anisotropy, such as 1D or 2D collapses, the resolution required in order to adequately describe the physical system strongly depends on direction. To solve this problem, we introduce the concept of *anisotropic smoothing tensor* H. In this new formalism, the spherical zone of influence of a given particle is replaced by a triaxial ellipsoid. Each ellipsoid is defined by a triad of mutually perpendicular vectors, the semimajor axes of the ellipsoid, which have three components each. We refer to this ensemble of nine components as the *H-tensor* of the particle. The H-tensors are dynamically

evolved by the ASPH code using the components of the deformation tensor $\partial v_i/\partial x_j$ to follow the local deformation and vorticity of the flow. In ASPH, the 3D Gaussian kernel is given by

$$W_3(\mathbf{r}_{ij}, \mathbf{H}) = W_1(x', h_1)W_1(y', h_2)W_1(z', h_3) = \left(\frac{e^{-x'^2/h_1^2}}{\pi^{1/2}h_1}\right)\left(\frac{e^{-y'^2/h_2^2}}{\pi^{1/2}h_2}\right)\left(\frac{e^{-z'^2/h_3^2}}{\pi^{1/2}h_3}\right), \quad (3)$$

where $\mathbf{r}_{ij} = \mathbf{r}_i - \mathbf{r}_j$, W_1 and W_3 are the 1D and 3D Gaussian kernels, respectively, $h_1 = |\mathbf{h}_1|$, $h_2 = |\mathbf{h}_2|$, and $h_3 = |\mathbf{h}_3|$ are the semimajor axes of the ellipsoid, and x', y', and z' are the projections of $\mathbf{r}_{ij}$ along each of these axes. This technique has three strong advantages over standard SPH:

1) The resolving power of the SPH equations in regions with strong anisotropy can be increased by orders of magnitudes.

2) The H-tensors track the motion of the flow, and consequently each particle keeps roughly the same set of neighbors for many timesteps. This implies that the usually costly nearest neighbor search need be done only occasionally instead of at every time step, resulting in a large speed-up of the algorithm.

3) Caustics and shocks in the flow can be predicted to occur whenever a particle's H-tensor ellipsoid shrinks along one of its axes enough to make the volume go to zero. This forms the basis for our shock tracking algorithm described below.

Shock Tracking and Artificial Viscosity. The evolving H-tensors track the local deformation of the fluid. Without artificial viscosity, particle crossing would occur whenever a particle encounters a shock, and this would result in an "inversion" of the H-tensor for this particle, with the shortest axis shrinking to negative values. The ASPH method makes use of this phenomenon by turning artificial viscosity on *only* for particles whose H-tensor is about to undergo this inversion. This automatically restricts artificial viscosity to just those fluid particles which are actually encountering a shock.

4. The Pancake Collapse Test Problem

We focus in what follows on a tough test problem, that of the gravitational collapse of a 1D, plane wave density fluctuation in a universe comprised of baryons and collisionless dark matter. This is the cosmological pancake problem, in which an initially linear amplitude density fluctuation grows to nonlinear amplitude, forms a caustic in the dark matter distribution located in the plane of symmetry of the pancake and strong accretion shocks, one on each side of this central plane, followed by continued infall, phase-mixing of the dark matter, and radiative cooling of the shocked baryon-electron plasma. Detailed, 1D numerical solutions for this problem already exist[2,4,5], as do approximate analytical solutions, for comparison.

The initial condition is just that of the growing mode of a 1-D, sinusoidal, adiabatic, plane wave, cosmological density fluctuation of comoving wavelength λ_p in an Einstein-de Sitter universe. The perturbed comoving position x of the mass element whose unperturbed

position is q is given by

$$x = q - \frac{\delta(t_i)}{2\pi}\lambda_p \sin\frac{2\pi q}{\lambda_p} \tag{4}$$

at initial time $t = t_i$ at which the amplitude $\delta(t_i) \ll 1$. The initial density is given by

$$\rho = \frac{\bar{\rho}(t_i)}{1 - \delta(t_i)\cos 2\pi q/\lambda_p}, \tag{5}$$

and initial peculiar velocity is given by

$$v_x = -\frac{H_0}{2\pi}\lambda_p\left(\frac{a_i}{a_0}\right)^{-3/2}\delta(t_i)\sin\frac{2\pi q}{\lambda_p}, \tag{6}$$

where a is the cosmic scale factor, $a_i = a(t_i)$, $a_0 = a_{\text{present}} = 1$, H_0 is the Hubble constant, and $\bar{\rho}(t_i)$ is the mean density at t_i. The perturbation is given to both the baryonic and dark matter components. A dark matter caustic forms at $x = q = 0$ and shocks form just outside the center, at time t_c and $a = a_c = a_i[\delta(t_i)]^{-1}$ For the pancake test runs, we have taken $\Omega_{tot} = 1 = \Omega_{DM} + \Omega_b$, with $\Omega_{DM} = \Omega_b = 0.5$, $h = 0.5$, $a_i = 1/28$, $a_c/a_i = 4$, and units in which $\lambda_p = 1$. Radiative cooling is neglected.

4.1. 1D Results: ASPH vs. Standard SPH

We begin with a 1D, plane-symmetric version of both the ASPH and the standard SPH methods, in which the particles may be thought of as plane sheets, and gas and dark matter particles are of equal mass. These 1D calculations are pseudo-3D, in the sense that the smoothing length for standard SPH varies according to $h \propto \rho^{-1/3}$, while the ASPH tensor H component along the collapse direction (evolved using $\partial v/\partial x$) varies as $h_x \propto \rho^{-1}$. We consider a range of gas particle numbers, N_{gas} (i.e. resolutions), distributed across one period λ_p, in a sequence of independent runs.

Figure 1 shows a comparison of the 1D SPH and ASPH results plotted against the analytical solution for a time-slice $a/a_c = 1.5$, well past the time of shock and caustic formation. This figure shows how the two flaws of SPH described above (inability to track a 1-D planar collapse with an isotropic $h \propto \rho^{-1/3}$, and artificial viscosity preheating) force the method to require an enormous value of N_{gas} to match the analytical solution while ASPH does better with very much smaller N_{gas}.

4.2. 2D Results: ASPH vs. Standard SPH

Our ASPH method, in principle, can automatically identify and adjust to accommodate a pancake collapse and shocks along *any* direction, not known *a priori*. Testing this fully requires at least a 2D calculation (i.e. in this case (x,y) Cartesian coordinates). We, therefore, reconsider the pancake problem, except we solve it using a 2D version of the SPH and ASPH methods, respectively, and solve the gravitational force problem by using a standard Particle-Mesh (PM) method[6,7]. For 2D SPH, the smoothing length $h \propto \rho^{-1/2}$.

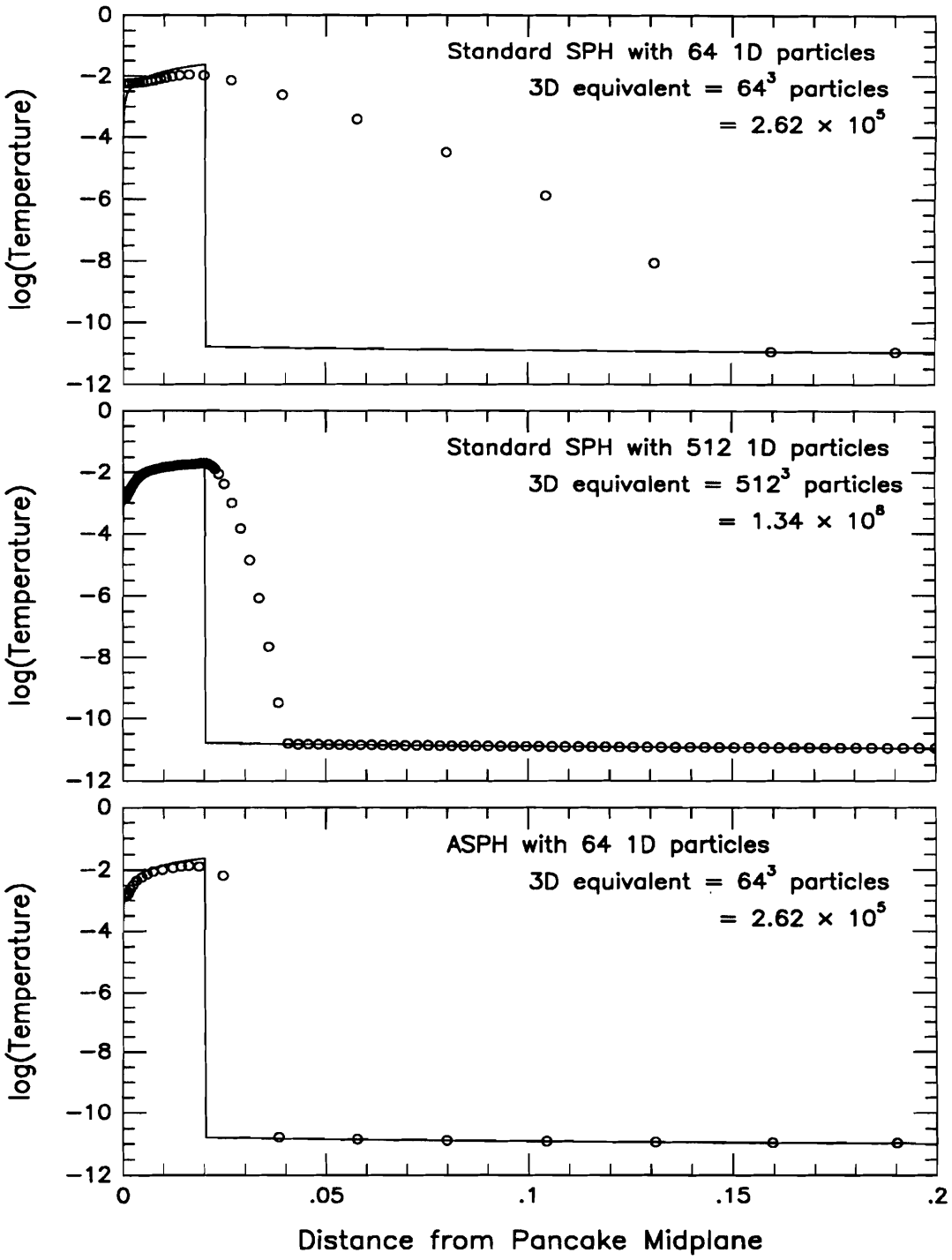

Figure 1. Gas temperature (in computational units) for 1D pancake test at $a/a_c = 1.5$. Numerical results (open circles) and exact 1D solution (solid line).

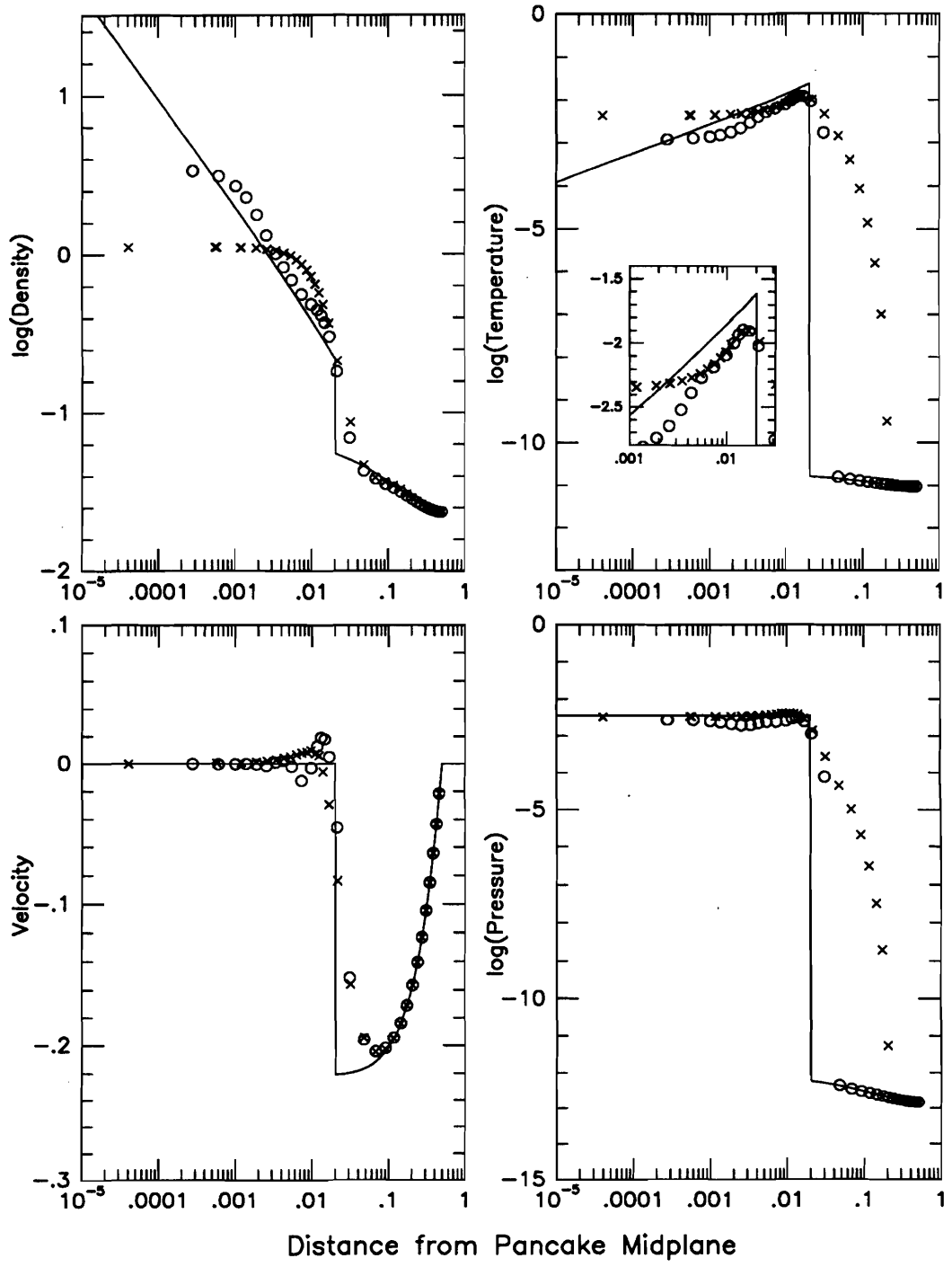

Figure 2. 2D tilted, shifted pancake test at $a/a_c = 1.5$. ASPH (open circles), SPH (crosses), and exact solution (solid line). Computational units.

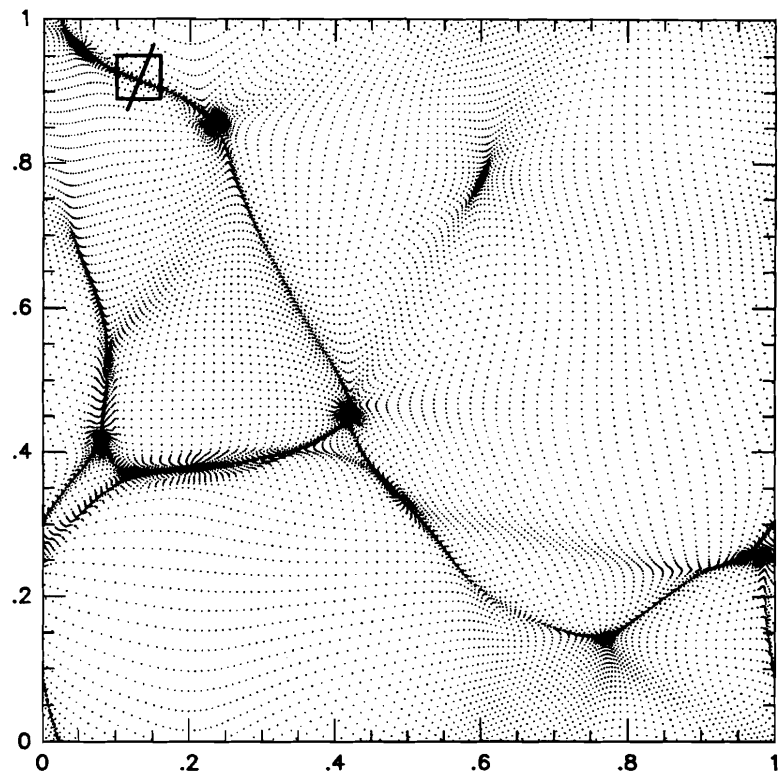

Figure 3. 2D HDM results at $z = 0$: ASPH gas particle positions. Small box is enlarged in Fig. 4.

Tilted, Shifted Pancake We consider a square box with periodic boundary conditions and one edge-on pancake of wavelength $\lambda_p = L_{box}/\sqrt{2}$, oriented with its symmetry plane (*i.e.* density maximum) at 45° with respect to the walls of the computational box, and shifted away from the box center. We take $N_{gas} = N_{DM} = 64 \times 64 = 4096$ particles of each type (equal mass particles) with initial positions displaced by the perturbation away from the same square uniform lattice. This is designed to test that ASPH can adjust to follow the anisotropic collapse of the pancake regardless of its orientation. (*NOTE:* In this case, given the 45° angle of tilt, there are now only 22 gas particles per row perpendicular to the pancake to resolve the flow for each side of the pancake central plane.) The PM calculation uses a square lattice grid with $128 \times 128 = 16,384$ cells per box.

Results are shown at time-slice $a/a_c = 1.5$, along with the exact solution, in Figure 2. The ability of ASPH to match the analytical solution with *no preheating* and with the slope of the postshock profiles in agreement over orders of magnitude of position and density variation is in contrast to the standard SPH results which show preheating, shock spreading, and poor postshock profile fitting.

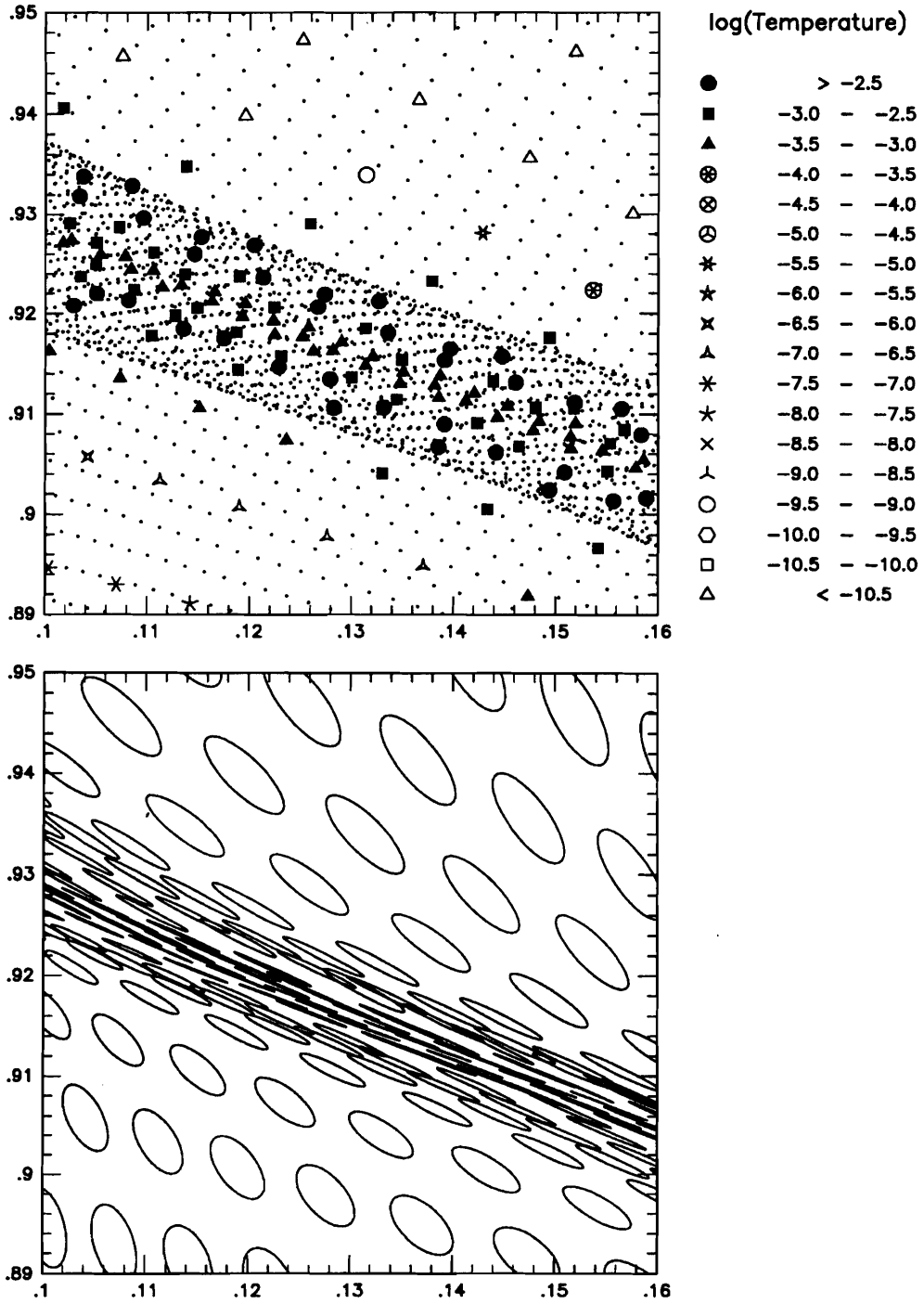

Figure 4. Zoom-in enlargement of small box in Fig. 3. (Upper panel) Particle positions: HDM (small dots), gas (other symbols) with temperature bin indicated [computational units= $T(^\circ K)/2.57 \times 10^9$]. (Lower panel) H-tensor ellipses (axes scaled by 0.15)

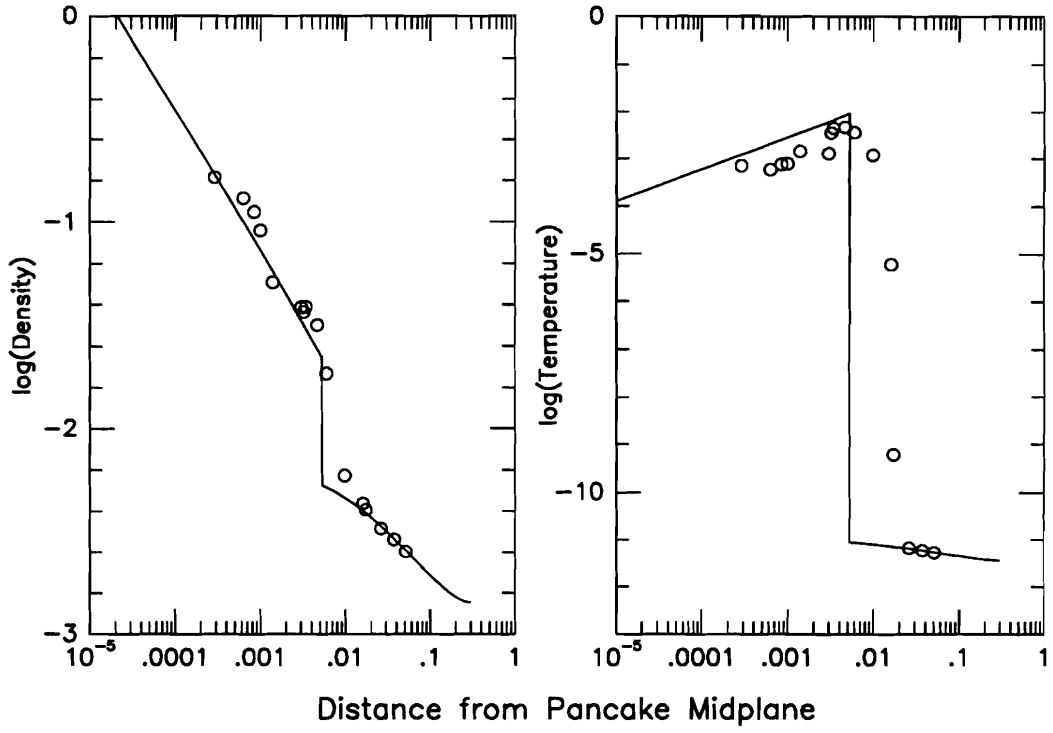

Figure 5. Line "cut" thru pancake in Figs. 3 and 4, with gas particles (open circles) and analytical pancake solution (line), for one side of pancake central plane only. Distance units have $L_{box} = 1$.

5. 2D, Cosmological Hydro Simulation Using ASPH/PM: HDM Universe

We apply our ASPH method in 2D to simulate the growth of large-scale structure in a universe dominated by HDM, with density fluctuations given by Gaussian random noise based upon a Harrison-Zel'dovich primordial power spectrum ($n = 1$) with amplitude fixed by the COBE satellite detection of CMB anisotropy. The HDM power spectrum we use is $P(k) = < \delta_k^2 > = Ak^{n+1}10^{-1.5(k/k_D)}$, where $k_D = 2\pi/\lambda_D$, λ_D = damping length $\cong$ $13\,\mathrm{Mpc}(\Omega h^2)^{-1}$ (i.e. 2D power spectrum is same as 3D, but multiplied by $2k$—equal rms $\delta\rho/\rho$ for equal fluctuation scale length).

We take $h = 0.5, \Omega = 1, \Omega_{DM} = 0.9375, \Omega_b = 0.0625, N_{particles} = 512{\times}512 = 262,144$ total, $N_{gas} = 128 \times 128 = 16,384$ particles, with initial positions perturbed away from a uniform square lattice in a simulation box of side $L_{box} = 200\,\mathrm{Mpc}$ with 1024×1024 PM cells and periodic boundary conditions, at initial redshift $z_i = 24$. The initial density fluctuations are represented as the superposition of plane wave perturbations with random phases including all wavevectors which satisfy periodic boundary conditions with dimensionless wavenumber $k = L_{box}/\lambda$ in the range $1 \leq k \leq 256$. Radiative cooling is neglected.

5.1. Results: ASPH resolves Pancakes

We show gas particle positions at $z = 0$ in Figure 3, indicating the prevalence of pancake-like structure (in 2D, lines are edge-on pancakes), along with edge-on filaments and clusters at pancake intersections. The small box in the upper left corner, centered on one such edge-on pancake, is enlarged in Figure 4, showing both dark matter and gas particles in the top panel and the anisotropic smoothing tensor ellipses surrounding each gas particle in the lower panel. The temperature symbols for the gas indicate that the two pancake shocks are sharply resolved with a separation of order 10^{-2} times L_{box} with the hottest immediate postshock particles forming two plane layers between which are cooler, previously shocked gas particles, as expected for pancake collapse. To show how well the ASPH results resolve pancake shocks like this, including the postshock profiles, we have plotted in Figure 5 the temperature and density for particles located in a "cut" thru the pancake, in a band centered on the line segment shown inside the small box in Figure 3, drawn perpendicular to the pancake central plane, versus logarithmic distance measured perpendicular to that plane. We use the gas velocity profile in the numerical data to identify the location of the shock, the pancake wavelength, and the bulk peculiar drift velocity of the entire pancake, and plot the exact 1D solution for such a pancake against the numerical results. The numerical results provide a remarkably good match to this idealized 1D pancake solution, indicating that ASPH succeeds in resolving pancake shocks on scales of order 10^{-3} times L_{box}! This required fewer than 40 gas particles per dimension per pancake. Our simulation took approximately 10 hours of Cray Y-MP time running at 153 Megaflops.

References

[1] Peebles, P. J. E. 1993, *Principles of Physical Cosmology* (Princeton: Princeton University Press).
[2] Shapiro, P. R., Struck-Marcell, C. 1985, *Astrophys. J. Suppl.* **57:** 205.
[3] Monaghan, J. J. 1992, *Ann. Rev. Astron. Astrophys* **30:** 543.
[4] Shapiro, P. R., Struck-Marcell, C., Melott, A. L. 1983, *Astrophys. J.* **275:** 413.
[5] Bond, J. R., Centrella, J., Szalay, A. S., Wilson, J. R. 1984, *Mon. Not. Roy. Astron. Soc.* **210:** 505.
[6] Hockney, R. W. & Eastwood, J. W. 1981, *Computer Simulation Using Particles* (New York: McGraw-Hill).
[7] Villumsen, J. V. 1989, *Astrophys. J. Suppl.* **71:** 407.